

## Design and Simulation of Robust Controller for Flexure Stage Based Piezo-Actuated Nanopositioning Device

Sheilza Jain<sup>1</sup>, Maneesha Garg<sup>2</sup> and Akhilesh Swarup<sup>3</sup>

<sup>1</sup>*Electronics Engineering Department,  
YMCA University of Science and Technology, Faridabad-121006, India*

<sup>2</sup>*Humanities and Applied Science Department,  
YMCA University of Science and Technology, Faridabad-121006, India*

<sup>3</sup>*Electrical Engineering Department,  
National Institute of Technology, Kurukshetra-132119, India  
sheilzajain1@gmail.com, Garg\_maneesha@yahoo.com*

### Abstract

*The rapid growth and rise in applications of nanotechnology demand investigation and control of matters at nanometer or subnanometer scale. The fundamental component of nanotechnology is the nanopositioning device, which can be used to scan or position the sample precisely at nanometer or subnanometer scale. Besides fine resolution, high precision positioning and long travel range, many applications of nanotechnology require fast positioning system. To achieve these requirements, design of high precision and high bandwidth nanopositioning device is needed. To achieve nanoscale precision over nanoscale, nanopositioning stage driven by stack piezoelectric actuator is widely used in applications such as atomic force microscope (AFM) and scanning tunneling microscope (STM). This paper presents open loop time and frequency response characteristics of piezoelectric actuator based nanopositioner. The transient response characteristics and stability margins of this device can be improved by using feedback control law. This paper shows that substantial improvement in operating speed and position precision has been achieved using a feedback controller. The presence of hysteresis is the significant challenge in the use of piezoelectric actuator for nanopositioning applications. A successfully designed control system must be able to maintain stability margins and performance level, even in the presence of uncertainties/ nonlinearities in system dynamics and/or in the working environment to a certain degree. To meet these requirements, this paper synthesizes robust and optimal H-infinity controllers for a system having hysteresis non-linearities. Simulation results using MATLAB are given to validate the proposed controller for nanopositioning device. Further, a comparative analysis of different types of proposed controllers is also described.*

**Keywords:** *Nanopositioners, piezoelectric actuators, feedback controller, robust controllers*

### 1. Introduction

The rapid rise and growth of research in the field of nano science and nanotechnology has directly affected the applications on nanotechnology including nano machining, scanning probe microscopy, microlithography and nano metrology [1-4]. Manipulation at nanoscale by using atomic force microscopy (AFMs) is well established and has a great potential as a process for prototyping nano-devices and systems, for repairing structures built by other means; and for small batch manufacturing [5]. Scanning Tunneling Microscope (STM) [6],

Atomic Force Microscope (AFM) [7] and Scanning probe Microscope (SPM) [8] can be used to measure surface properties fundamentally changed research in many areas. Precise control, manipulation and interrogation at nanometer scale demand positioning system having nanometer or subnanometer resolution, *i.e.*, nanopositioner. Nanopositioners are the essential requirement in virtually all applications of nanotechnology and further research in the SPM based research area shall depend on the availability of highly precise nanopositioning devices [9].

Nanopositioners are the mechatronic device used to move and measure a probe, part, tool, sample or a device at desired position with subnanometer precision and accuracy. Nanopositioners must be able to resolve adjacent positions separated by less than a nanometer. Nanopositioners having desirable properties such as long travel range, greater mechanical robustness and ease of interrogation, can be used in the field of nano-fabrication, nano-mechanics, aerospace, astronomy, defense, biotechnology, information technology (data storage), chemical industries, photonics and test application in the semiconductor devices [9-11]. Nanopositioners are also required to manipulate atomic and molecular scale structure and to characterize surface properties of materials. Moreover, fast nanopositioners are important in applications such as manipulator's pick and place operation near a wall and filling a tank with fluid in minimum time without spilling over [12]. For instrumentation such as scanning probe microscope, optical microscope, profilometers, dual storage servo system of HDDs (Hard Disk Drives) and critical dimension measuring tools, ultra precise nanopositioning systems, sensors, actuators and motion controllers are the prime elements [9]. To achieve very high resolution, high bandwidth, and fast time response, a large number of nanopositioning device geometries have been proposed [13-16].

Distortion free imaging and accurate metrology applications demand development of closed loop control based on position sensing techniques for subnanometer and nanometer resolution [7]. In the area of micro and nanoscale systems, piezoelectric actuator (PA) is the most popular candidate used for actuation because of the very high resolution of the order of nanometer, high stiffness, mechanical simplicity, compact size and its versatility to be implemented over a wide range of applications [17-19]. But presence of inherent nonlinearities such as hysteresis, damping, drift and mechanical resonance, significantly reduces the achievable precision obtained using piezoelectric actuator; and also there are challenges in its design and control [17-21]. Because of aforementioned limitations, practical nanopositioning systems require feedback/closed loop controls to obtain satisfactory performance. Control system must be designed to reduce the tracking error and must guarantee a high precision positioning under variable operating conditions. The dynamic behavior of the system depends upon the control technique used. A variety of control techniques have been proposed to compensate the nonlinearities of piezo actuators (PAs) and to improve precision and speed of systems using PAs [22-26]. Nonlinearities of piezoelectric actuators and hysteresis can be compensated by using standard Proportional - Integral (PI) or Proportional - Integral - Derivative (PID) controllers in all the applications where high performance and accuracy are not critical constraints. Challenging problems of nanoscale control persists due to non - linear dynamics, actuators modeling uncertainties, instabilities and lack of robustness against external disturbances and sensor noise [26]. Use of PID controllers are not only costly but also potentially lead to bandwidth limitations and inefficiencies, so the solution of all above mentioned problems is the robustification control of nanopositioning system by designing robust controllers.

## 2. System identification and open loop characteristics

Nanopositioning is an important characteristic of a huge family of SPMs that has emerged since the invention of the STM and AFM. To achieve nanoscale precision, flexure based nanopositioning stage driven by stack piezoelectric actuators is widely used. Flexure based mechanism eliminates back-lash, friction and lubricant requirement for the device and provides precise, smooth and repeatable motions to fulfill the requirement of accurate nanoscale positioning. The nanopositioning system developed by S. Salapaka et al. [25] consists of a flexure system, an actuation system, a detection system, an evaluation system and a control system as shown in Figure 1.

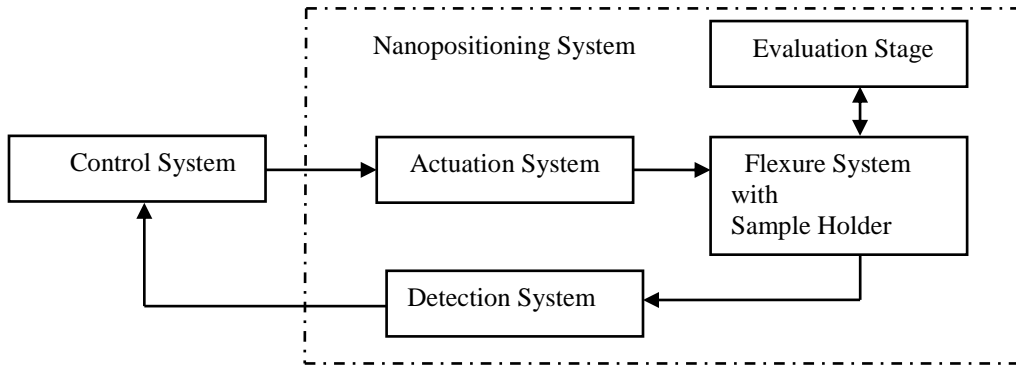


**Figure 1. Schematic Block Diagram of Nanopositioning System**

Generally, the nanopositioning stage is actuated by an assembly of piezoelectric stacks and voltage amplifier. This assembly is positioned in the slot of the flexure stage. The flexure stage consists of sample deforms under the application of force and thus provides motion to the sample. These forces are generated by piezo stack actuators and high voltage inputs are provided by the voltage amplifier. The motion of the sample is sensed and measured by the LVDT sensor. An AFM is also located above the sample holder to make AFM measurements simultaneously with the LVDT measurements. After proper control action, the amplified output of LVDT is applied to the piezoelectric stack, which leads to its deformation and impart motion to the flexure stage and hence to the sample. The magnitude of input to the amplifier is limited to be negative or less than 10 volts to avoid saturation of piezo stack arrangement. The actuator leads to a travel range of approximately 100 micrometers and the LVDT sensor used has resolution of about  $2\text{\AA}$  over 1KHz bandwidth [25].

Model of the device has been inferred by studying its frequency response over a specified bandwidth. For modeling, the device is operating in the linear region of its characteristics. Offset of the device to operate about the null position is -5V. The dynamics of the system can be approximated by fourth order transfer function given as [17, 25]

$$G(S) = \frac{9.7 \times 10^4 (s - (7.2 \pm 7.4i) \times 10^3)}{(s + (1.9 \pm 4.5i) \times 10^3)(s + (1.2 \pm 15.2i) \times 10^2)} \quad (1)$$

The pole zero location of the system depicts that this is a non-minimum phase (NMP) system consisting of one pair of complex conjugate zeros in the right half s-plane (RHP). RHP zeros pose limitations on the performance specifications of the device and control of NMP system requires special attention.

Poles and zeros of open loop system are symmetric about imaginary axis consisting of a pair of complex conjugate values. The presence of complex conjugate poles indicates the oscillatory response of the system. Pair of poles  $[-(1.9 \pm 4.5i) \times 10^3]$  having natural frequency of 4.88 KHz and damping ratio of 0.389 dictate the control input magnitude and are called short period modes. Pair of very lightly damped (damping ratio 0.0787) characteristic modes  $[-(0.120 \pm 1.52) \times 10^3]$  with lower value of natural frequency (1.52 KHz) are known as long period mode or dominant poles. All poles have negative real part, which implying that system is asymptotically stable from the stability criteria. The settling time of the transient response, speed of the system is governed by the dominant poles of the system. The damping ratio of dominant poles is very small and need controllers to improve the damping ratio and hence the phase margin.

Analysis of frequency response of nanopositioning device shows the phase margin of 27.2 degree at gain crossover frequency of  $1.61 \times 10^3$  rad/sec and gain margin of 4.63dB at phase crossover frequency of  $1.74 \times 10^3$  rad/sec. It is found that there is very small variation in the frequency response of the system from DC signal to AC signal. Time response analysis gives Settling Time: 0.0335 seconds and maximum overshoot of 83.6016 which is very large and must be avoided using control techniques.

### 3. Controller Design and Implementation

The open loop performance characteristics of the device are not satisfactory because of having high value of settling time, rise time and maximum overshoot. The main objectives of the control designs are high precision tracking with high bandwidth, compensating the adverse effects of nonlinearities presents in the system and achieving robustness of the closed loop system against model uncertainty. A schematic diagram of Single Input Single Output (SISO) feedback loop for single stage nanopositioning device is shown in Figure 2.

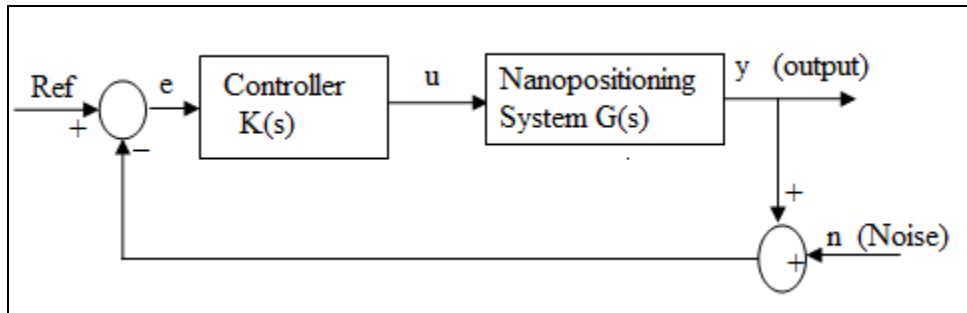


**Figure 2. Closed loop system for SISO Nanopositioning Device**

In Figure 2, Ref is the reference signal and y is the actual output of the plant. (e) is the error given by  $(\text{Ref}-y) = (S.\text{Ref} - Tn)$  where sensitivity function  $S=1/(1+G(s)K(s))$  is the transfer function from Ref to e error and complementary sensitivity function  $T = 1 - S$  is the transfer function from Ref to y (output).  $K(s)$  is the transfer function of the controller which has to be designed. The primary objective of the controller is to design a system with a high precision positioning and high bandwidth tracking capability with robustness to the uncertainty in the operating condition.

Let the SISO linear control system is described by state equation

$$\dot{x}(t) = Ax(t) + B_1 w(t) + B_2 u \quad (2)$$

$$z(t) = C_1 x(t) + D_{11} w(t) + D_{12} u(t) \quad (3)$$

$$y(t) = C_2 x(t) + D_{21} w(t) + D_{22} u(t) \quad (4)$$

Where  $w(t)$  is the disturbance vector

$u(t)$  is the control input vector

$z(t)$  is the error vector

$y(t)$  is the output or observation vector and

$x(t)$  is the state vector.

$H_\infty$  robust control approach is applied to design a controller for non-minimum phase nanopositioning system. The foremost step for the designing of the  $H_\infty$  controller is the formation of generalized or augmented plant  $P(s)$ . The interconnection of augmented plant  $P(s)$  with controller  $K(s)$  are shown in Figure 3.

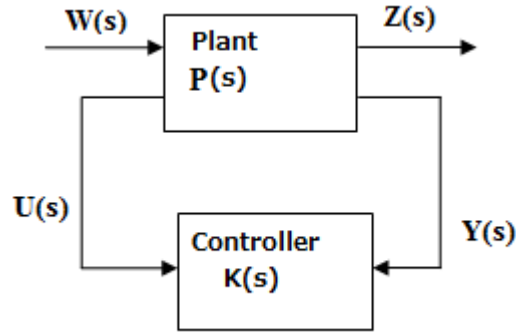


**Figure 3. Interconnection of Augmented Plant  $P(s)$  with controller  $K(s)$**

The augmented plant  $P(s)$  that includes weights  $W(s)$  and  $G(s)$  can be described by block transfer function matrix as

$$P(s) = \begin{bmatrix} P_{11}(s) & P_{12}(s) \\ P_{21}(s) & P_{22}(s) \end{bmatrix} = \begin{bmatrix} A & B_1 & B_2 \\ C_1 & D_{11} & D_{12} \\ C_2 & D_{21} & D_{22} \end{bmatrix} = \begin{bmatrix} W_P & -W_P G \\ 0 & W_T G \\ 0 & W_U \\ 1 & -G \end{bmatrix} \quad (5)$$

For a linear controller having transfer function  $K(s)$  connected from  $y$  to  $u$ , the transfer function of the closed loop system from  $w$  to  $z$  after interconnection of  $P(s)$  with  $K(s)$  is given as

$$F_l(P, K) = P_{11} + P_{12} K(s) (1 - P_{22} K(s))^{-1} P_{21} \quad (6)$$

and is known as Linear Fractional Transformation (LFT) of the interconnected system.

In the design of robust controller, the objective is to choose a controller  $K(s)$  which makes closed loop system stable and minimizes  $\|F_l(P, K)\|_\infty$  [27-29] such that

$$\|F_l(P, K)\|_\infty < 1 \quad (7)$$

Based on equation (6) three types of robust controllers can be designed such that

$$a) \ H_2 \text{ optimal controller : } \min_{K(s)} \|F_l(P, K)\|_2 ; \quad (8)$$

$$b) \ H_\infty \text{ optimal controller: } \min_{K(s)} \|F_l(P, K)\|_\infty ; \quad (9)$$

$$c) \ \text{The standard } H_\infty \text{ robust controller: } \|F_l(P, K)\|_\infty < \gamma \quad (10)$$

To achieve the performance objectives, weighting transfer functions are designed to shape the sensitivity function  $S$ , complementary sensitivity transfer function  $T$  and control transfer function  $KS$ . The closed loop system with weighted output is shown in Figure 4. Here the exogenous input  $W$  is the reference signal Ref and measured output  $Z$  is the error signal  $e$ . the transfer function  $G$ ,  $W_p$ ,  $W_T$  and  $W_u$  must be proper or bounded as  $S \rightarrow \infty$  [28].  $W_p$  is the weight on  $S$  which is used to describe the performance objectives of the closed loop system for good tracking bandwidth.  $W_T$  is the weight on  $T$  which shapes the performance objectives of the noise rejection/ uncertainty or to describe the robustness of the closed loop system.  $W_u$  is the weight on  $KS$  so as to bound control signal under the saturation limits. The weighted outputs are given as

$$\begin{bmatrix} Z_1 \\ Z_2 \\ Z_3 \end{bmatrix} = \begin{bmatrix} W_p e \\ W_T y \\ W_u U \end{bmatrix} = \begin{bmatrix} \text{weighted output error} \\ \text{weighted system output} \\ \text{weighted control input} \end{bmatrix}$$

The transfer function  $W_p$  is chosen to have high gain at low frequency and low gain at high frequency to emphasize tracking error in a low frequency range. The transfer function  $W_T$  must have high gain at high frequencies to make complementary sensitivity function  $T$  small at high frequencies. The weighting transfer function  $W_u$  is chosen constant so as control signal avoid saturation of actuator [30, 31].

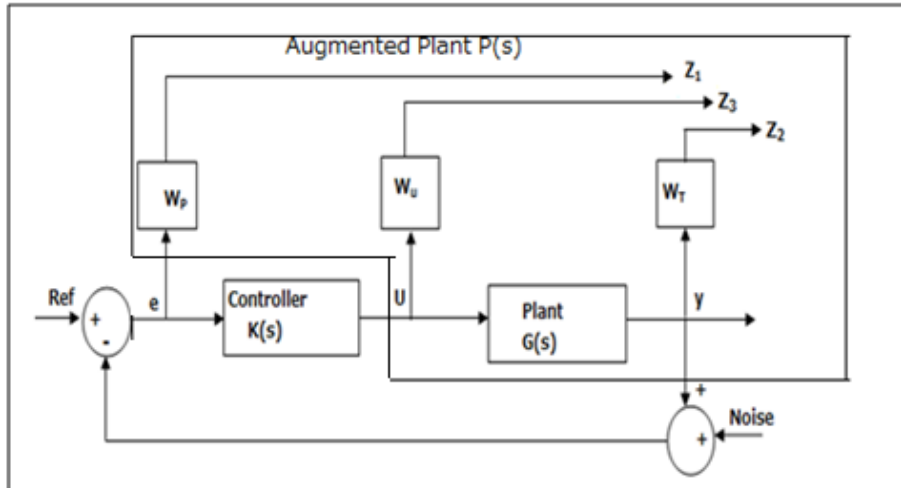


Figure 4. Closed loop system with weighted output

The  $H_\infty$  disturbance attenuation performance requirement can be written as:

$$\|S(j\omega)W_p(j\omega)\|_\infty < 1 \text{ and it is known that} \\ \|G\|_\infty = \max|G(j\omega)| \quad \forall \omega \quad (11)$$

So the above equation can be written as

$$|S(j\omega)| < |W_p(j\omega)|^{-1} \quad (12)$$

Therefore performance objectives impose a bound on the sensitivity function S.

Similarly, a closed loop system is stable with respect to the uncertainty if and only if it satisfies the condition defined by

$$\|W_T(j\omega)T(j\omega)\|_\infty < 1 \quad (13)$$

Hence  $W_T$  imposes a bound on the complementary sensitivity function T.

The optimal  $H_\infty$  controller must be designed to satisfy the criteria

$$\|W_pS, W_TT, W_uKS\|_{\max} \leq 1 \quad (14)$$

And robust  $H_\infty$  controller must be designed by satisfying

$$\|W_pS, W_TT, W_uKS\|_{\max} \leq \gamma \quad (15)$$

The constant gamma  $\gamma$  represents the desired performance level of the closed loop system. Gamma  $\gamma$  equals to 1 or less indicates that the controller constraints are met.

#### 4. Controller implementation and simulation

A To design  $H_\infty$  controller for the system described by equation 1, let us consider that the transfer function for weighted outputs are

$$w_p(s) = \frac{0.1667s + 2827}{s + 2.827}, \quad W_T(s) = \frac{s + 235.6}{0.01s + 1414}, \quad w_u = 1$$

Typical Frequency response of  $W_p$  and  $W_T$  is shown in Figure 5.

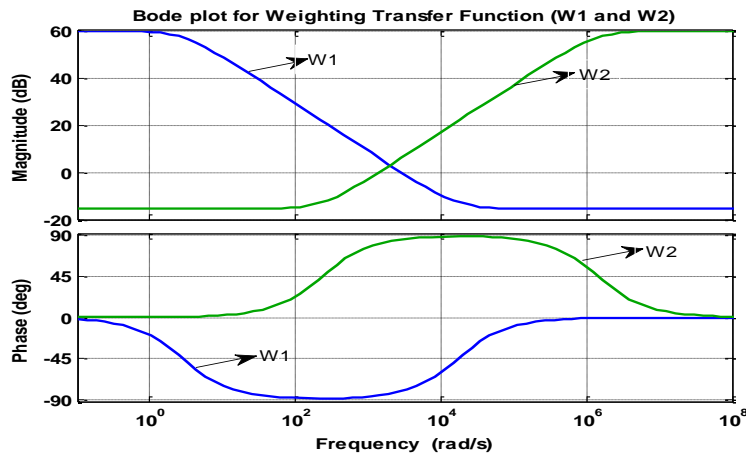


Figure 5. Bode Plots for Weighting Transfer Function

The Implementation of weighting transfer functions  $W_P$ ,  $W_T$  and  $W_u$  on the system described by equation 1 results into augmented plant  $P(s)$ . The simulation of augmented plant  $P(s)$  using MATLAB can be used to design different types of H controller.  $H_2$  optimal controller  $K(s)$  for augmented plant  $P(s)$  designed by using the formulae described by Doyle, *et al.*, [29] can be expressed in terms of pole, zero and gain as

$$\frac{2.807(s+1.414 \times 10^6)(s^2+240s+2.325 \times 10^6)(s^2+3800s+2.386 \times 10^7)}{(s+1318)(s+2.827)(s^2+514.2s+3.273 \times 10^6)(s^2+3825s+2.395 \times 10^7)} \quad (16)$$

By using feedback gain of 0.1665, the locations of closed loop poles of the nanopositioning system are:

$$\begin{aligned} & -1.91 \times 10^3 \pm 4.50 \times 10^3 i \\ & -1.90 \times 10^3 \pm 4.50 \times 10^3 i \\ & -2.61 \times 10^2 \pm 1.76 \times 10^3 i \\ & -1.20 \times 10^2 \pm 1.52 \times 10^3 i \\ & -7.53 \times 10^1 \\ & -1.24 \times 10^3 \end{aligned}$$

It can be seen that all the poles of closed loop system has negative real part indicating that system is asymptotically stable from the stability criteria.

$H_\infty$  robust controller for the partitioned plant  $P(s)$  is synthesized using  $\gamma$  gamma iteration technique. By computing the smallest value of gamma  $\gamma$ , a 6<sup>th</sup> order suboptimal  $H_\infty$  controller with transfer function given by equation (10) is obtained.

$$\frac{1893.248(s+1.414 \times 10^6)(s^2+240s+2.325 \times 10^6)(s^2+3800s+2.386 \times 10^7)}{(s+4.125 \times 10^5)(s+2.827)(s^2+1712s+4.591 \times 10^6)(s^2+3802s+2.282 \times 10^7)} \quad (17)$$

The smallest value of gamma obtained is 4.59 which is slightly greater than the H infinity norm of closed loop system. The closed loop poles of system for feedback gain of 0.1665 are located in left half s- plane having negative real part.

Under the same robust control setup mentioned above, the synthesis of  $H_\infty$  optimal controller using  $\gamma$  iteration technique results in 6<sup>th</sup> order transfer function of the controller is given as

$$\frac{331.2343(s+1.414 \times 10^6)(s^2+240s+2.325 \times 10^6)(s^2+3800s+2.386 \times 10^7)}{(s+7.18 \times 10^4)(s+2.827)(s^2+1699s+4.633 \times 10^6)(s^2+3815s+2.282 \times 10^7)} \quad (18)$$

Gamma-Iteration technique computes optimal H-Infinity controller for a given partitioned plant  $P(s)$  via the improved Loop-Shifting two-Riccati formulae. The optimal "gamma" obtained using this synthesis method is  $\gamma = 0.266$  which is less than unity.

The time and frequency responses for the above mentioned robust controllers are given in Figure 6.

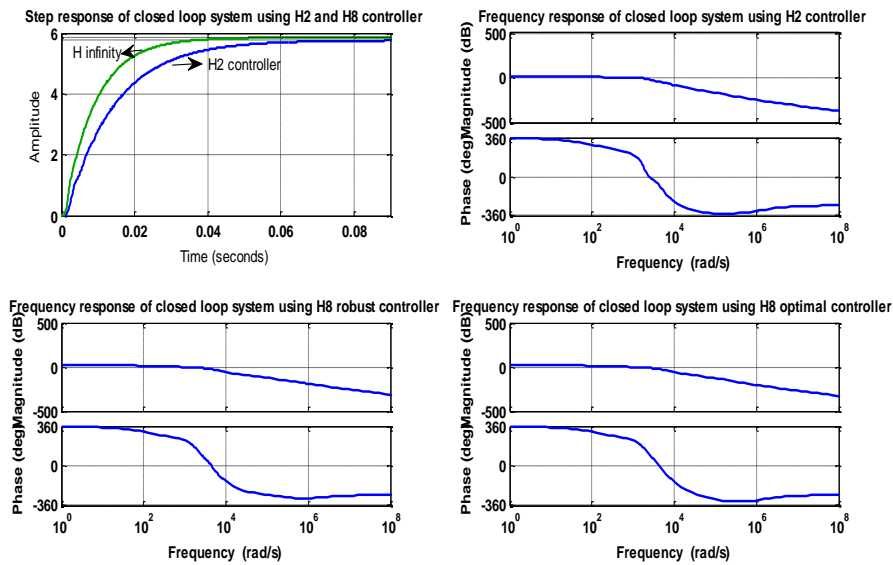


**Figure 6. a) Time response of robust controllers; b) Frequency response of H2 controller; c) Frequency response of  $H^\infty$  suboptimal controller; d) Frequency response of  $H^\infty$  optimal controller**

The summary of the closed loop characteristics of the time and frequency responses for the different types of robust controller for nanopositioning device are tabulated in Table 1 given below:

**Table 1. performance characteristics of robust H controller**

Type of controller	Rise time (sec.)	Settling Time (sec)	Maximum Overshoot	Gain margin (db)	Phase margin (degree)	Bandwidth (Hz)
$H_2$ controller	0.0291	0.0532	0	6.58	69.33	75
$H_\infty$ Robust	0.0184	0.0338	0	4.16	66.86	118.39
$H_\infty$ Optimal	0.0184	0.0339	0	4.12	66.81	117.89

As depicted from Table 1, the feedback connection of different types of robust controllers with the nanopositioning device improves the system performance effectively. The problem of maximum overshoot is completely solved by the use of robust controller. Moreover transient response characteristic shows remarkable improvement in rise time and settling time as compared to the open loop characteristics. Optimum value of stability margins, phase, gain margins and increase in bandwidth of the nanopositioning system are observed.

## 5. System Robustness

By Use of robust controller in the feedback loop of nanopositioning system not only the transient and stability performance characteristics are improved but also the closed loop system becomes robust enough to provide good performance and stability over the uncertainty such as parameter changes, actuator saturation and model uncertainty. Robust controller results into very high disturbance rejection with high stability margins under any

operating conditions. Robustness of the system can be measured by singular values. Disturbance attenuation is determined by the singular values of  $S(j\omega)$ . Thus a disturbance attenuation performance specification can be written as:

$$\sigma(S(j\omega) \leq |W_p^{-1}(j\omega)| \tag{19}$$

Where

$|W_p^{-1}(j\omega)|$  is the desired disturbance attenuation factor.

Singular values of  $S(j\omega)$  for different frequencies  $\omega$  are given by singular values plot of  $S(j\omega)$ . Similarly singular values plot of  $T(j\omega)$  is used to determine stability margins for system uncertainty. Smaller is the value of  $\sigma$ , greater will be the stability margin. Figure 7 plots the singular value plot of  $S(j\omega)$  and  $T(j\omega)$  for different types of robust controller.

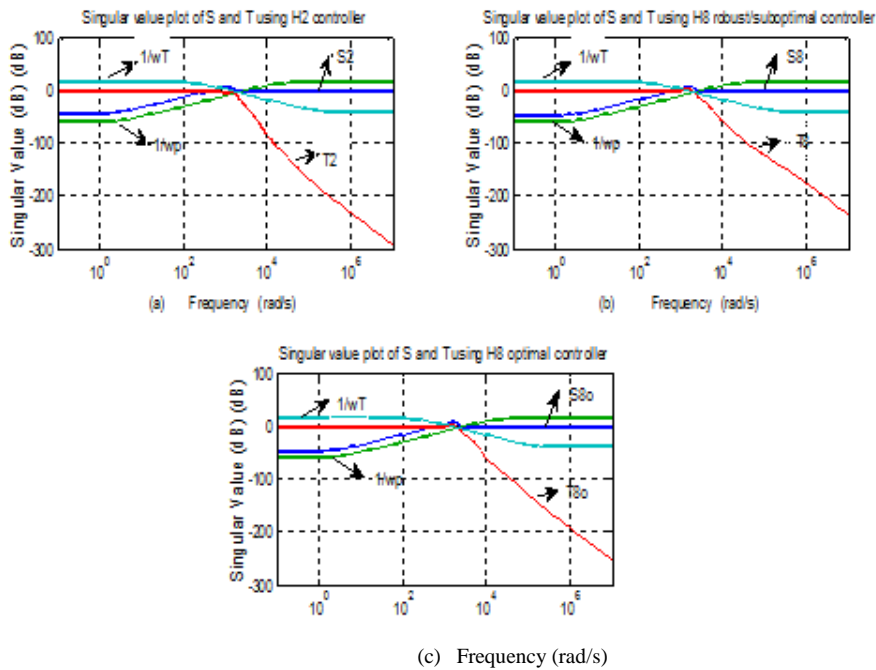


**Figure 7. singular value plot for sensitivity transfer function S and complementary sensitivity transfer function T: (a) H<sub>2</sub> controller; (b) H<sub>∞</sub> robust/suboptimal controller; (c) H<sub>∞</sub> optimal controller**

Singular value of the sum of sensitivity function and complementary sensitivity function is a good measure of robustness. The less is the value of maximum singular value, better is the control or stability margins. As seen from the Figure 7, the singular value of sensitivity function and complementary sensitivity function for H<sub>2</sub> controller, H<sub>∞</sub> robust/suboptimal controller and H<sub>∞</sub> optimal controller of the nanopositioning system lies below the zero gain for the operating range of frequency (120Hz).

## 6. Conclusion

In this paper a flexure stage based nanopositioning device has been identified and its open loop characteristics have been analyzed. Optimal H<sub>2</sub> controller has been designed and

analyzed. By using gamma iteration technique,  $H_\infty$  robust/suboptimal controller and  $H_2$  optimal controllers have been designed and implemented on the nanopositioning system. Problem of maximum overshoot of open loop system has been overcome by the use of robust controller. Remarkable improvement in stability margins and transient response has been observed by the implementation of robust controllers on the nanopositioning system. Robustness indicator plots (Singular value plots) have shown that robustification against perturbations/uncertainty has been achieved for the operating frequency range of 120Hz.

## References

- [1] I. Fujimasa, "Micromachines: a new era in mechanical engineering", Oxford, U.K. Oxford University, Press, (1996).
- [2] B. Bhushan, "Handbook of Micro/nanotribology", Boca Raton CRC, (1999).
- [3] B. Bhushan, "Handbook of Nanotechnology", New York Springer, (2004).
- [4] T. R. Hicks and P. D. Atherton, "The Nanopositioning Book: Moving and Measuring to better than a nanometer", London U.K. ISTE, (2000).
- [5] B. Mokaberri, Aristides and A. G. Requicha, "Compensation of scanner creep and hysteresis of AFM Nanomanipulation", IEEE transaction on automation Science and Engineering, (2005).
- [6] G. Bining and H. Rohrer, "Scanning Tunneling Microscope", Scientific American, vol. 253, (1986), pp. 50-56.
- [7] K. K. Leang, Q. Zou and S. Devasia, "Feedforward Control of Piezo actuators in Atomic Force Microscope System", Asian Journal of Control, vol. 29, no. 1, (2009), pp. 72-80.
- [8] S. M. salapaka and M. V. Salapaka, "Scanning probe Microscope", IEEE Control System Magazine, vol. 28, no. 2, (2008), pp. 65-83.
- [9] S. Devasia, E. Eleftheriou and S. O. R. Moheimani, "A Survey of control issues in nanopositioning", IEEE transaction on Control System Technology, vol. 15, no. 5, (2007), pp. 802-823.
- [10] A. A. Tseng, S. Jou, A. Notargiacomo and T. C. Chen, "Recent development in tip based nanofabrication and its roadmap", journal of nanoscience and nanotechnology, vol. 8, no. 5, (2008), pp. 2167-2186.
- [11] B. Potsaid, J. T. Wen, M. Unrath, D. watt and M. Alpay, "High Performance Motion tracking control for electronic manufacturing", Journal of Dynamic System, Measurement and control, vol. 129, (2007), pp. 767-776.
- [12] A. Ferreira and C. Mavroidis, "Virtual Reality and haptics for nanorobotics", IEEE robot Automation magazine, vol. 13, no. 3, (2006), pp. 78-92.
- [13] H. Shakir and W. -J. kim, "Multiscale control for nanoprecision positioning systems with large throughput", IEEE transaction on control system technology, vol. 15, no. 5, (2007).
- [14] S. Sebastian and S. M. Salapaka, "Design methodology for robust nanopositioning", IEEE transaction on control system technology, vol. 13, no. 6, (2005).
- [15] G. schitter, K. J. astrom, B. Demartiny, P. J. Thurner and K. L. turner, "Design and modeling of high speed AFM scanner", IEEE transaction on control system technology, vol. 15, no. 5, (2007).
- [16] K. K leang and A. J. fleming, "High speed serial- kinematics AFM scanner: Design and Drive consideration", Asian journal of control, vol. 11, no. 2, (2009).
- [17] T. Chang and X. Sun, "Analysis and control of monolithic piezo-electric nano-actuator", IEEE transaction on control system technology, vol. 9, no. 1, (2006).
- [18] A. Sudjana, K. K. Tan, s. K. Panda and T. H. lee, "Design, Modeling and control of piezoelectric actuators for intracytoplasmic sperm injection", IEEE transaction on control system technology, vol. 15, no. 5, (2007), pp. 879-890.
- [19] S. jain, M. garg and A. Swarup, "Identification and Performance improvement of nanopositioning devices", International journal of applied engineering research, vol. 6, no. 5, (2011), pp. 627-631.
- [20] S. O. Moheimani, "Accurate and fast nanopositioning with piezoelectric tube scanner: Emerging trend and challenges", Review of Scientific Instruments, vol. 79, no. 7, (2008).
- [21] G. schitter and A. stemmer, "Identification and open loop tracking control of piezoelectric tube scanner for high speed scanning probe microscopy", IEEE transaction on control system technology, vol. 12, no. 3, (2004).
- [22] C. V. Newcomb and I. Flinn, "Improving the linearity of piezoelectric ceramic actuators", Electron letter, vol. 18, no. 11, (1982), pp. 442-444.

- [23] N. W. Hagood, W. H. Chung and A. V. Flotow, "Modeling of piezoelectric actuator dynamics for active structure control", Journal of Intelligent materials system and structure, vol. 1, (1990), pp. 327-354.
- [24] Y. K. Yong, S. S. Aphale and S. O. r. Moheimani, " Design, Identification and Control of a flexure based XY stage for fast nanoscale positioning", IEEE transaction on nanotechnology, vol. 8, no. 1, (2009), pp. 46-54.
- [25] S. Salapaka and A. Sebastian, "Control of Nanopositioning Devices", IEEE Conference on Decision and Control, Hawaii, USA, (2003), pp. 2644-2649.
- [26] P. Ge and M. Jouaneh, "Tracking control of piezoelectric actuators", IEEE Transaction on control system technology, vol. 4, no. 3, (1996), pp. 209-216.
- [27] S. Skogestad and I. Postlethwaite, "Multivariable feedback control", New York, John Wiley & Sons, (2000).
- [28] K. Glover and J. C. Doyle, "state space formulae for all stabilizing controllers that satisfy an  $H_\infty$  norm bound and relations to risk sensitivity", System and control letters, vol. 11, (1988), pp. 167-172.
- [29] J. C. Doyle, K. Glover, P. Khargonekar and B. Francis, "State space solution to standard  $H_2$  and  $H_\infty$  control problems", IEEE Transaction on Automatic control, vol. 34, no. 8, (1989), pp. 831-847.
- [30] J. Dong, S. M. Salapaka and P. M. Ferreira, "Robust MIMO control of a parallel Kinematics Nanopositioner for High resolution high bandwidth tracking and repetitive tasks", IEEE conference on Decision and Control, USA, (2007), pp. 4495-4500.
- [31] D. -W. Gu, P. H. Petkov and M. M. Konstantinov, "Robust Control Design with MATLAB", Springer-Verlag London Limited, (2005).

## Authors



**Sheilza Jain** did B.Tech in Electronics and Communication Engineering from Kurukshetra University, India and M.Tech with specialization in Control System from Maharishi Dayanand University, India. Presently she is working as Assistant Professor in Electronics Engineering Department at YMCA UST Faridabad and is pursuing Ph.D in Nano-positioning from Maharishi Dayanand University. Her interest area includes control system, analog circuits.



**Dr. Maneesha Garg** did her Ph.D (Physics) in 2002 from Kurukshetra University, India. After that she worked as Research Associate granted by CSIR, in NIT Kurukshetra for 4 years. She has 18 publications in national, international journals and more than 30 papers in conferences to her credit. Presently she is working as Assistant Professor in Humanities and Applied Science Department, YMCA UST, Faridabad and guiding 4 scholars for their research work.



**Prof. A. Swarup** received B.E. in Electrical Engineering from MN Regional Engineering College, Allahabad and M.Tech. with specialization in Control Systems from IT-BHU, Varanasi. He obtained his Ph.D. from IIT Delhi in the area of Robotic Control. He is serving at National Institute of Technology Kurukshetra since 1981. Presently he is working as Professor of Electrical Engineering and Dean (Research & Consultancy). His areas of research interest are Robotic Control, Robust Control and Navigational Control.

He is Senior Member of IEEE and Member of its Control System Society. Also, he is Life Member of Systems Society of India (SSI) and Indian Society for Technical Education (ISTE).